Estimation of Cotton Leaf Area Index under Verticillium Wilt Stress Based on UAV Multispectral & Optimization Algorithm

Yujing Tian
Tarim University
Jiaojiao Hui
Tarim University
Nannan Zhang
Tarim University
Mingdeng Shi
Tarim University
Li Wang
Tarim University
Qingsong Jiang
120070002@taru.edu.cn
Tarim University

Research Article

Keywords: leaf area index, verticillium wilt stress, UAV multispectral, Optimization algorithm

Posted Date: April 30th, 2026

DOI: https://doi.org/10.21203/rs.3.rs-9387581/v1

Additional Declarations: No competing interests reported.

Estimation of Cotton Leaf Area Index under Verticillium Wilt Stress: Based on UAV Multispectral & Optimization Algorithm

Yujing Tian [a,b], Jiaojiao Hui [a,b], Nannan Zhang [a,b], Mingdeng Shi [a,b], Li Wang [a,b] and Qingsong Jiang [a,b,*]

a College of Information Engineering, Tarim University, Alar 843300, China; 107572230551@stumail.taru.edu.cn (Y.T.); 120210106@taru.edu.cn (J.H.); zhangnannan@taru.edu.cn (N.Z.); smdeng@taru.edu.cn (M.S.);15609324483@163.com (L.W.)

b Key Laboratory of Tarim Oasis Agriculture (Tarim University), Ministry of Education, Alar 843300, China

*Correspondence: 120070002@taru.edu.cn

Abstract: Verticillium wilt is one of the main factors hindering cotton yield increase, the more severe the disease, the more severe the yield loss. In order to achieve early detection and prevention of Verticillium wilt, this study investigated cotton plants naturally affected by Verticillium wilt in the field. We analyzed the cotton canopy multispectral data under the stress of Verticillium wilt and the leaf area index (LAI) data collected from the ground. Due to the low prediction accu-racy of traditional empirical models, this paper selected three different back propagation BP neural network models with 5, 10, and 15 hidden layer nodes (hln) and optimized them using four intelligent swarm algorithms: genetic algorithm (GA), particle swarm optimization (PSO), spotted hyena algorithm (SHO), and improved spotted hyena algorithm (ISHO) to estimate the cotton LAI under the stress of Verticillium wilt. Finally, BP algorithm with different node number of hidden layer was optimized by comparing four intelligent swarm optimization al-gorithms to estimate LAI of cotton under verticillium wilt stress. The findings indicated that GA-BP (hln15) was the best in the GA-BP algorithm; In the PSO-BP algorithm, PSO-BP (hln10) performed best; In the SHO-BP model, SHO-BP (hln5) had the highest model performance; In the ISHO-BP model, ISHO-BP (hln5) is the best, with a determination coefficient(R2), root mean square error(RMSE), and prediction accuracy(PA) of 0.952, 0.235, and 89.30%, respec-tively; The estimation results of ISHO-BP (hln5) model can better represent the distribution of Verticillium wilt plants than GA-BP (hln15), PSO-BP (hln10), and SHO-BP (hln5), and its estimation error range is (-0.8,0.5). Therefore, the application of ISHO-BP (hln5) model pro-vides a new method for estimating cotton LAI under pest and disease stress, and also provides technical support to meet the diversified needs of cotton farmers to increase their income and national economic development.

Keywords: leaf area index; verticillium wilt stress; UAV multispectral; Optimization algorithm

1. Introduction

Cotton has an irreplaceable role in the development of global trade and economy (Zhang et al., 2018), and cotton also occupies an important position in China's agricultural economy (Liu et al., 2015). Xinjiang accounts for more than 90 percent of the country's cotton output (Chen et al., 2006). Cotton diseases are one of the main factors restricting cotton production, the most serious and widely distributed disease and pest of cotton is Verticillium wilt (Huanget al., 2004), known as the "cancer" of cotton (Chen et al., 2010).With the continuous increase in cotton planting area, the disease broke out on a large scale in various cotton planting areas in China (Lai et al., 2014), causing a loss of 100000 tons of cotton in 1993 alone (Ma et al., 2007). Later, disasters occurred frequently in the Yellow River Basin (Ma et al., 1994), resulting in economic losses of up to 1.2 billion yuan (Jian et al., 2003). Since 2009, about 2.667 million hectares of cotton planting areas in China are affected by Verticillium wilt every year (Zhang et al., 2013;

Aziguli et al., 2016). Last several years, there has been a large-scale outbreak of Verticillium wilt disease in the Tahe River Basin in southern Xinjiang. Especially in 2018, there was a large-scale outbreak of cotton wilt disease in the Alar Reclamation Area, which severely affected over 36% of cotton fields (Zhao et al., 2021) and caused serious economic losses to local cotton farmers.

LAI is an important part of the study of terrestrial ecological processes, which can quantitatively describe the changes of leaf density and growth at the vegetation level (Waston et al., 1947). Verticillium dahliae reduces cotton LAI by blocking xylem vessels, secreting toxins, and inducing water stress, directly impairing leaf function. Simultaneously, it suppresses photosynthesis, disrupts hormone balance, and depletes defense resources, leading to leaf yellowing, abscission, and reduced new leaf growth. Canopy structure deterioration further exacerbates disease cycling(Nie et al., 2024). The LAI defined by Monteith is not applicable to non-flat-leaf plants (Smith et al., 1990). On this basis, in order to make LAI more inclusive, it was further defined as the vertical projected area of leaves per unit area, but the projected area mainly depended on the shape of plant canopy (Monteith et al., 2013). Therefore, the LAI defined by Chen et al. included the definition of broadleaf vegetation and the characteristics of coniferous vegetation (Chen et al., 1992). For relatively complex terrain (Maria et al., 2008), vegetation area defined by LAI can be transformed into each other through projection relationship (Gonsamo et al., 2008; Gao et al., 2015). Direct measurement method is destructive to plants and consumes a lot of manpower, resources and time, so it is not suitable for general data collection (Tan et al., 2008). Dense vegetation canopy data were collected by indirect measurement method (Wilson et al., 1960).

Due to the strict requirements of spatial and temporal resolution of cotton plants under verticillium wilt stress, traditional satellite remote sensing technology has been unable to provide high-quality data to meet the actual needs (Zou et al., 2006)]. Therefore, it is necessary to use UAV sensing technology to estimate cotton LAI under verticillium wilt stress. More and more studies have been accomplished to estimate crop LAI using UAV (Yang et al., 2019; Li et al., 2022; Ji et al., 2022). For example, Shao et al. established a relationship model between vegetation index and LAI during the whole growth period of wheat under different irrigation conditions by using UAV and random forest method (Shao et al., 2020). Later, researchers began to use drone remote sensing technology to estimate and study crop pests and diseases to reduce farmers' production costs and relieve ecological pressure. Wang et al. estimated the LAI of wheat rust by UAV (Wang et al., 2023). Jing et al. constructed a study on estimating the severity of cotton single leaf blight based on hyperspectral image features (Jing et al., 2023). Dilixiati constructed a cotton pest monitoring algorithm based on multi-spectral remote sensing images (Dilixiati et al., 2021). Therefore, spectral imaging data can be used to construct cotton leaf area estimation model under verticillium wilt stress. On this basis, due to the high cost of hyperspectral remote sensing technology, the UAV multi-spectral remote sensing technology was used to estimate cotton LAI under verticillium wilt stress.

BP neural network is a mathematical tool for nonlinear prediction that can store and learn numbers of mapping relationships between input and output patterns without the need to reveal and describe these mapping relationships beforehand. Its network can learn the knowledge hidden in the data to provide predictive accuracy (Qi et al., 1998). Xin et al used BP neural network and meteorological data to generate spatiotemporal continuous LAI time series, and the result was that BP algorithm had better performance (Xin et al., 2021). Hong and Tang et al used BP neural network to estimate forest LAI, and the prediction accuracy of BP algorithm was relatively high (Hong et al., 2022; Tang et al., 2021) .Xue et al used BP neural network to estimate high-resolution leaf area index, and the model had a high accuracy(Xue et al.,2019). Therefore, this paper used BP neural network model to predict cotton leaf area index under verticillium wilt stress, which can learn the tacit knowledge between VI and LAI, so as to improve the estimation accuracy of cotton leaf area index under verticillium wilt stress.

The optimization algorithm is a mathematical tool used to find the best solution to a given problem in order to find the best solution (optimal value). Optimization algorithms include particle swarm optimization (PSO), genetic algorithm (GA), and so on. These algorithms iterate over the search space to constrain the objective function and obtain the optimal solution. GA is a search model that uses the evolution law of the biological world to find the best value (Li et al., 2007) to solve the optimization problem. PSO is a simulated search algorithm derived from a simplified social model, inspired by the graphical simulation of beautiful scenes of flocks of birds (Bonah et al., 2020). Various intelligent swarm optimization algorithms have been developed (Saremi et al., 2017). Compared with the traditional optimization algorithm, its convergence speed and optimization effect show the best results. The Spotted hyena algorithm (SHO) has higher problem-solving ability (Zhong et al., 2023).While the improved Spotted Hyena algorithm (ISHO) has better hunting ability and can find the optimal solution faster. ISHO algorithm is widely used in image segmentation, hyperspectral band selection and other fields (Dai et al., 2022). In some previous studies, the SHO-BP model was used to predict runoff, and its prediction accuracy was better than that of the SHO-SVM and PSO-BP algorithms (Li et al., 2021). Previous studies have verified that the hyena algorithm can improve the prediction accuracy of BP neural networks in predicting runoff. The researchers also optimized the BP neural network based on the improved spotted hyena algorithm, and built the estimation algorithm of forest LAI estimation. The estimation effect of ISHO-BP is more accurate than that of BP neural network (Tao et al., 2020).

In summary, the objectives of this study are: (1) to develop an estimation model for the LAI of cotton under Verticillium wilt stress; (2) to compare the performance differences of BP neural network models optimized by GA,PSO, SHO, and ISHO with varying numbers of hln in LAI prediction; (3) to explore the accuracy and stability of the ISHO-BP estimation model, thereby providing a novel approach for LAI estimation under biotic stress and offering technical support to enhance cotton yield and meet the demands of national economic development.

2. Materials and Method

2.1. Sample

The study area is the 10 Tuan cotton experimental field in Alar City, Xinjiang, which is naturally affected by verticillium wilt. The test area is about 14000 square meters. Its geographical coordinates are 40°37'3 "north, 81°20'39" East. Tahe No. 2 cotton variety was taken as the research object in this study. The growth period was about 135 days without water control or fertilization. The sowing method was 13-hole seeding, and the sowing date was April 3. As shown in Figure 1.

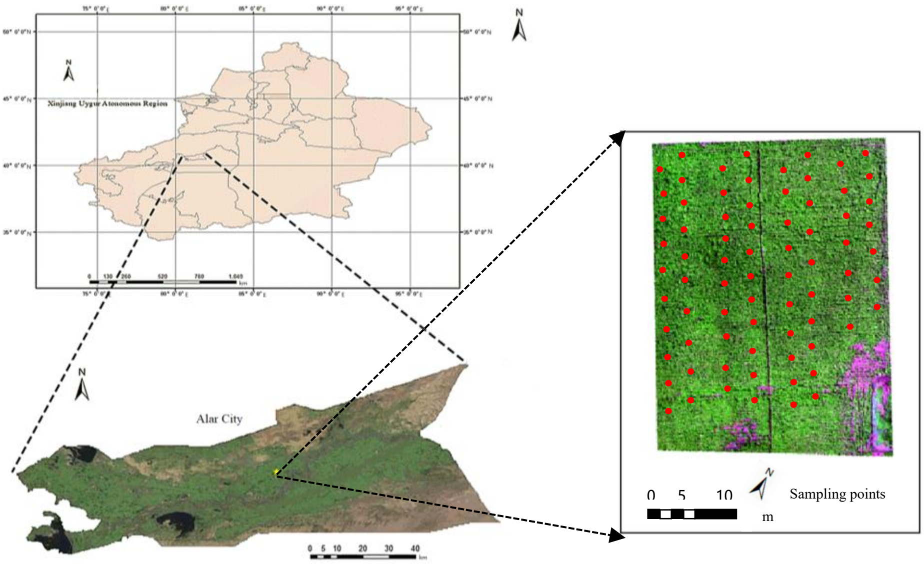

Figure 1. Geographical location of the experimental field.

2.2. UAV Image Acquisition and Pre-Processing

Cotton plots affected by natural verticillium wilt were selected as test areas, and the test area data were collected when verticillium wilt occurred in cotton fields. The data was collected on August 31and September 14, to ensure sufficient light and minimize data errors. Clear and windless weather was selected for data collection, and the solar light intensity was relatively stable during the period with good visibility. The data collection time was generally around 11:00-14:00, and unmanned aerial vehicles were used. The flight altitude is 25m, the ground resolution is 3cm, the margin is 5m, and the takeoff speed is 5.3m/s. In order to ensure effective stitching of remote sensing images in the later stage, the lateral overlap rate and heading overlap rate in the route are both 80%. Before planning the route, it is necessary to ensure that the unmanned aerial vehicles in the route area are not affected by high-voltage power lines, trees, buildings, and signal towers. When collecting data, the multispectral camera lens should be vertically downward and capture six bands: near infrared1, red, green, blue, red edge, and near infrared2. The individual images captured by UAV remote sensing systems have limited spatial coverage. Therefore, image stitching preprocessing is required to generate large-scale orthomosaic images of the experimental area. In this study, Pix4D mapper software was utilized for stitching the UAV-acquired multispectral remote sensing imagery.

Vegetation index (VI) is a combination of spectral features obtained from different bands of multispectral remote sensing images, and is an important theoretical parameter that reflects crop growth information, providing multidimensional support for accurate LAI prediction (Zhang et al., 2025a). Crop leaves exhibit strong absorption in the visible and red light spectral bands while demonstrating high reflectance in the near-infrared (nir) region. Consequently, various VI can be derived through mathematical combinations of spectral data from different bands. These VIs are typically constructed based on plant-sensitive spectral bands. For instance, NDVI effectively distinguishes vegetated areas from other land cover types by utilizing the differential reflectance between red and nir bands. Additionally, NDVI provides valuable information regarding crop health status and canopy coverage (Feng et al., 2025). NDRE, calculated using the red edge and NIR bands, offers more sensitive indicators of nitrogen content levels and plant health status(Zhang et al., 2025b). Building upon previous research and considering the spectral band configurations of UAV-mounted sensors along with LAI estimation requirements, this study selected eight broadband-reflectance vegetation indices as multivariate input variables for model construction. The selected indices include: NDVI, Green Normalized GNDVI, NDRE, RVI, DVI, RDVI, RERDVI, and OSAVI.

Table 2. The selected VI used in this study.

VI	Formula	Reference
NDVI	$(\mathrm{R_{nir}} - \mathrm{R_{red}})/(\mathrm{R_{nir}} + \mathrm{R_{red}})$	(Gitelson et al.,1996)
GNDVI	$(R_{nir} - R_{green})/(R_{nir} + R_{green})$	(Fitzgerald et al.,1975)
NDRE	$(R_{nir} - R_{red-edge})/(R_{nir} + R_{red-edge})$	(Pearson et al.,1972)
RVI	R_{nir}/R_{red}	(Zheng et al.,2020)
RDVI	$(R_{nir} - R_{red})/(R_{nir} - R_{red})^{0.5}$	(Gao et al.,2023)
RERDVI	$(R_{nir} - R_{red-edge})/(R_{nir} + R_{red-edge})^{0.5}$	(Hunt et al.,2011)
OSAVI	$(R_{nir} - R_{red})/(R_{nir} + R_{red} + L)(1 + L)$	(Jordan et al.,1969)
DVI	$R_{nir} - R_{red}$	(Rumelhart et al.,1986)

R_{nir}, R_{red}, R_{green} and $R_{red-edge}$ represent the reflectance of the near-infrared band, red band, green band, and red edge band, respectively; L represents adjusting parameters, usually taking a value of 0.16.

2.3. Ground Data Acquisition

This study also collected the leaf area index of cotton under the stress of Verticillium wilt on August 31 and September 14 on ground. During the test, the leaf area index of cotton under verticillium wilt stress was collected by LAI-2200C instrument, and 75 representative samples were selected, a total of 150 samples were studied. Each plot was selected for uniform growth, with a range of 2 × 2m. During the collection process, each LAI was measured with 1 A and 4 B, that is, the upper surface was measured at a distance of more than 4 times the leaf width above the cotton, and the lower surface was measured at the bottom of the cotton leaf. After collecting A and B, the instrument automatically calculates LAI.

2.4. BP Algorithm

Back propagation (BP) neural network model was first proposed by a scientific team led by Rumelhart and MCCelland (Nkongolo et al., 2022). BP neural network can store and learn a large number of mapping relationships. It is the mapping relationship of input-output mode and does not need to reveal the mathematical formula of this relationship beforehand.

2.4.1. GA

Genetic Algorithm (GA) (Huang et al., 2008), which is a stochastic search method, is an approach evolved based on the laws of biological evolution. It has the characteristics of robustness, efficiency and practicability. The accuracy of the training set under cross-validation (CV), which serves as a parameter for the fitness function of the genetic algorithm, is used to evaluate model performance, and the parameters of the BP model are optimized using the GA.

2.4.2. PSO

Particle swarm optimization (PSO) algorithm, an iterative technique grounded in swarm intelligence (Dhiman et al., 2017), was employed to optimize the parameters of the BP network. By leveraging its unique particle swarm mechanism, the algorithm continuously updated the fitness of particles until a global optimal solution was obtained.

2.4.3. SHO

The spotted hyena algorithm simulates the process of searching, surrounding, hunting, and attacking prey in a pack of hyenas to find the optimal solution (Li et al., 2021). The parameters of the BP model are optimized using the SHO model. Using the spotted hyena algorithm, continuously update the average value of the hyena's optimal solution set until obtaining the optimal individual position, which is the optimal solution.

2.4.4. ISHO

Improve the spotted hyena optimizer to train a BP neural network, where individual fitness values can be used to represent the distance between potential and optimal solutions in the solution space, i.e., the error. Use an improved spotted hyena optimizer instead of stochastic gradient descent to train a BP neural network, and gradually search for the optimal solution through iterations of the hyena population (Wang et al., 2017). When the algorithm ends, the optimal individual position vector is transformed and solidified into the weights and bias values of each neuron node in the BP neural network. The network training is completed, and the network model can output effective estimation values through input sample data, as shown in Figure 2.

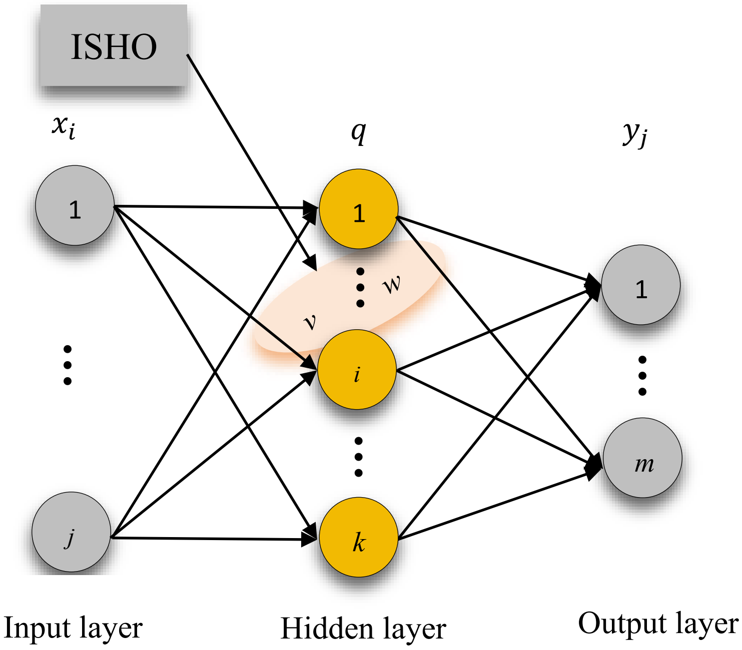

Figure 2. ISHO optimized BP neural network architecture.

To optimize the parameters of the BP neural network model, the parameter search time is reduced and improve prediction accuracy, optimization models such as GA, PSO, SHO and ISHO are used to enhance the ability of the BP neural network to invert cotton leaf area index under Verticillium wilt stress. And the prediction of BP neural network was completed in MATLAB R2023a software. Figure 2 shows the general completion process of optimizing the BP neural network model using GA, PSO, SHO, and ISHO optimization models. According to the flow chart, the data is first collected and preprocessed. Then, the data set was randomly divided into a training set and a test set in a 2:1 ratio. On this basis, four kinds of intelligent group optimization algorithms were proposed, namely genetic optimization algorithm, particle swarm optimization algorithm, hyena optimization algorithm, and improved hyena optimization method. When objective conditions are met, generate and output optimal parameters, and evaluate the BP neural network model using indicators such as R^2, RMSE, and PA. Finally, determine the estimation model for cotton leaf area index under Verticillium wilt stress.

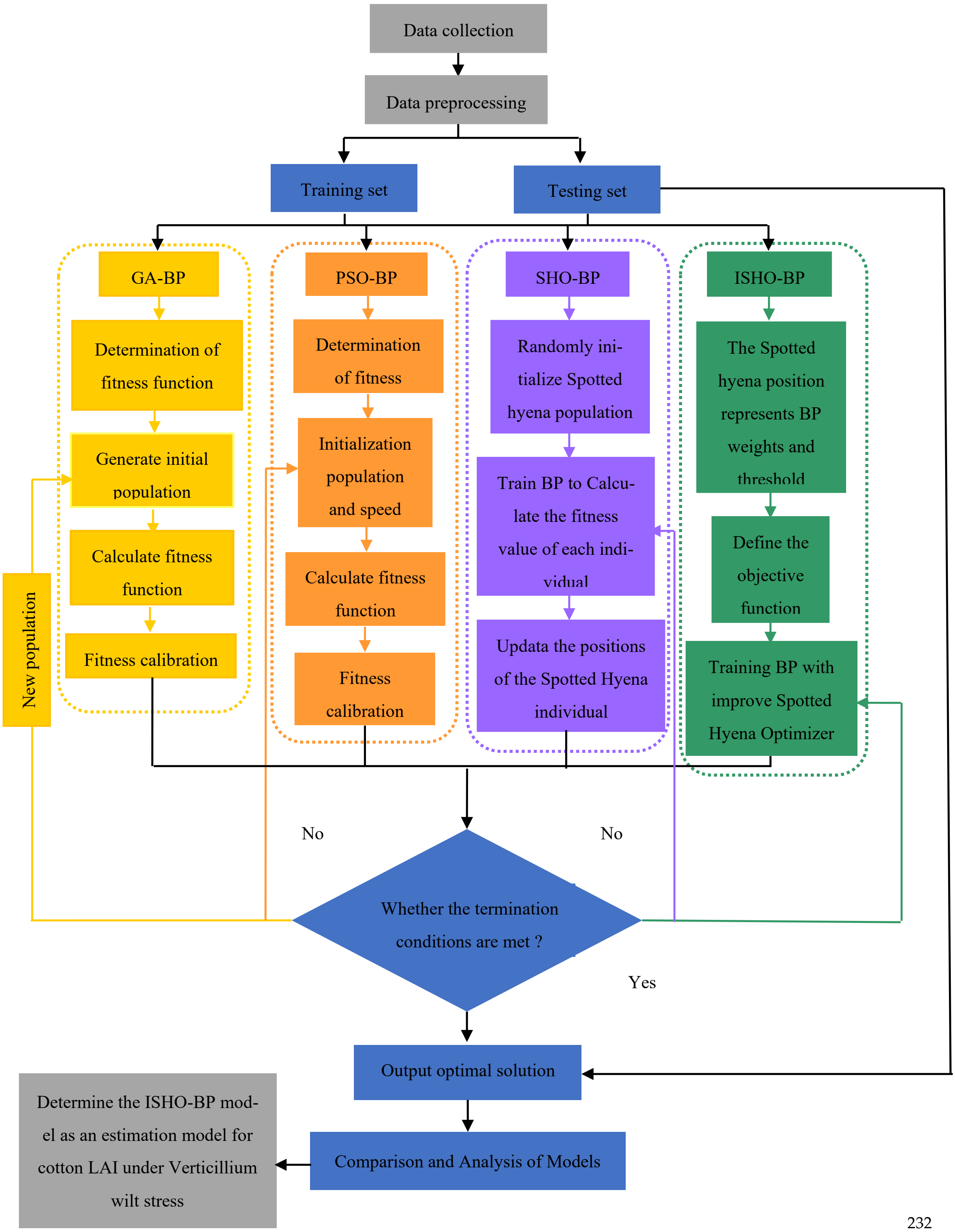

Figure 3. Process architecture of BP neural network algorithm optimized based on GA, PSO, SHO, and ISHO.

2.5. Evaluation of Model Performance

This study selected R^2, RMSE, and PA to evaluate the prediction accuracy and performance of the constructed algorithm. The closer the coefficient of determination is to 1, the better the explanatory power of the joint influence of the independent variables on the dependent variable in the fitting equation, and the higher the reliability and reference of the Estimation; RMSE is highly sensitive to outliers in measured values, reflecting the deviation between predicted and actual values. It can effectively represent the prediction accuracy of measurement. In this study, RMSE was used to verify the prediction accuracy of the algorithm established between cotton vegetation index and leaf area coefficient under Verticillium wilt stress. The smaller the value solved by RMSE, the smaller the data dispersion, indicating that the more accurate the data measurement and the higher the fitting accuracy. PA comprehensively reflects the accuracy of model prediction estimation (Zhao et al., 2022). The closer the prediction accuracy is to 100%, the higher the prediction accuracy of the constructed model in estimating leaf area index under Verticillium wilt stress. The model accuracy calculation is as follows:

$$R^2 = \frac{\sum_{i=1}^{n}(x_i-\bar{x})^2(y_i-\bar{y})^2}{\sum_{i=1}^{n}(x_i-\bar{x})^2\sum_{i=1}^{n}(y_i-\bar{y})^2}$$

$$RMSE = \sqrt{\frac{\sum_{i=1}^{n}(y_i-x_i)^2}{n}}$$

$$PA = \left(1-\frac{RMSE}{\bar{m}}\right)\times 100\%$$

x_{i} and y_{i} are the measured values and predicted values of cotton LAI, respectively. y_{i} and $\bar{y}$ are the ith predicted value and predicted average value of cotton LAI, n is the sample size, RMSE is the root mean square error, $\bar{m}$ and tests the average value of the sample data.

3. Results

3.1. Cotton VI under Verticillium Wilt Stress

VI is a combination of spectral features obtained from different bands of multispectral remote sensing images. By combining spectral data from different bands, different vegetation indices can be obtained. The ROI tool in ENVI software is used to extract vegetation indices from the combination and stitching of multispectral remote sensing images from unmanned aerial vehicles. In order to observe the distribution of VI more intuitively, as shown in Figure 3, statistical analysis and probability density distribution maps of eight cotton vegetation indices under Verticillium wilt stress are presented. Due to the high RVI values, they have been normalized. GuiiyiRVI has higher frequencies around 0.2 and 0.8, GNDVI and OSAVI have higher frequencies around 0.6-0.7, NDRE and RERDVI have higher frequencies around 0.3, RDVI has higher frequencies around 0.65, DVI has higher frequencies around 0.4 and 0.5, and NDVI has higher frequencies around 0.7 and 0.9. This graph shows the distribution range and differences of various vegetation indices under the stress of Verticillium wilt, providing a reference for observing the cotton canopy under the stress of Verticillium wilt.

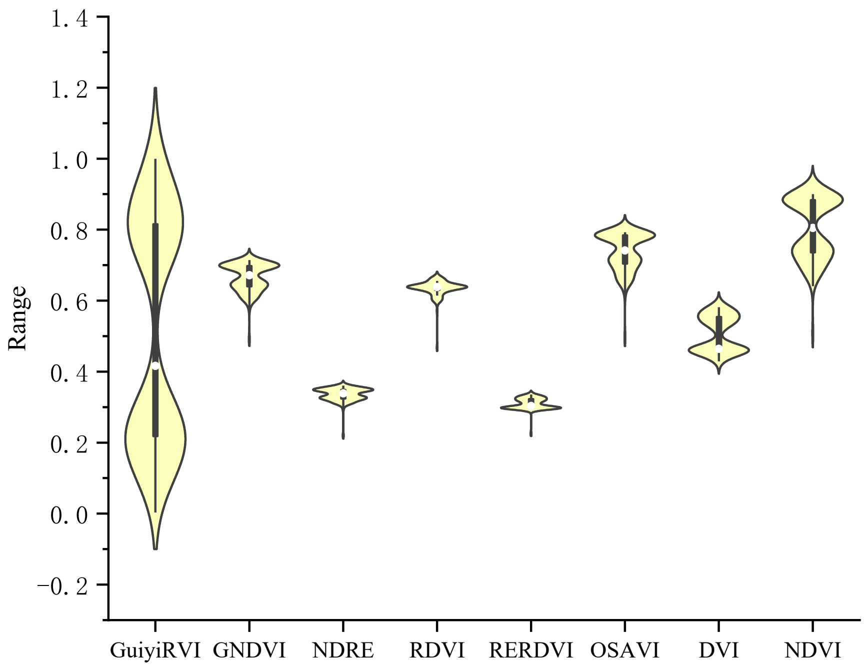

Figure 4. Statistical analysis and probability density distribution of cotton vegetation indices under eight types of Verticillium wilt stress.

3.2. Correlation Analysis of Cotton VI and LAI under Verticillium Wilt Stress

To demonstrate the correlation between cotton VI and LAI under Verticillium wilt stress, as shown in Figure 4, a correlation coefficient matrix was obtained between vegetation indices NDVI, GNDVI, NDRE, RVI, RDVI, RERDVI, OSAVI, DVI and LAI coefficient. *P<=0.05, which indicates significant correlation at a confidence level of 0.05. After checking the correlation coefficient significance test table, it was found that 8 vegetation indices were significantly correlated with LAI. Among them, NDVI, GNDVI, NDRE, RVI, RDVI, OSAVI were positively correlated with LAI, with correlation coefficients of 0.87, 0.83, 0.74, 0.82, 0.37, and 0.86, respectively. RERDVI, DVI, and LAI were negatively correlated, with correlation coefficients of -0.53 and -0.69, respectively. It can be seen that there is a close relationship between VI and LAI under the stress of Verticillium wilt. The potential of using these VI to invert cotton LAI under the stress of Verticillium wilt is enormous.

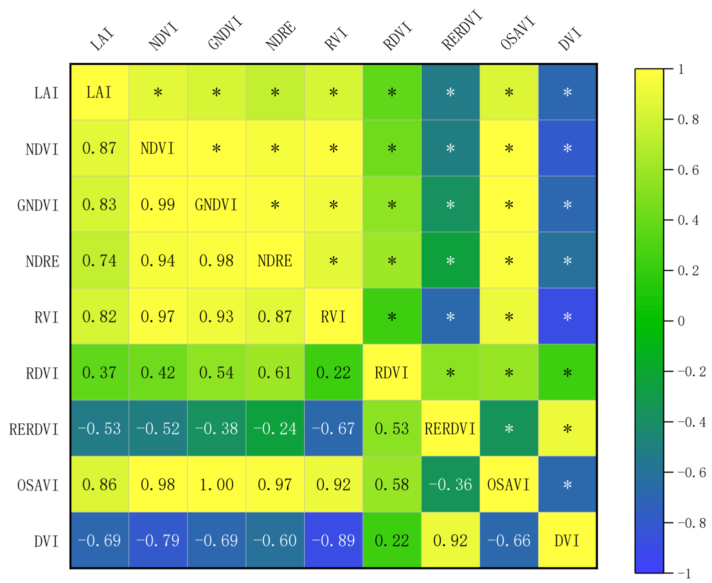

Figure 5. Correlation Matrix Between VI and LAI in Cotton Under Verticillium Wilt Stress.

3.3. Research on the Estimation Model of Cotton LAI under Verticillium Wilt Stress Based on Optimizing BP Algorithm Using Different Intelligent Swarm Algorithms

To compare the Estimation ability of different intelligent swarm optimization algorithms for cotton leaf area index under Verticillium wilt stress, we used GA, PSO, SHO and ISHO to optimize a BP neural network with 5 hln, as shown in Figure 7(a). Through the analysis of the convergence curve of experimental data, we found that the PSO-BP (hln5) model has the ability to converge quickly in the calculation of cotton LAI under Verticillium wilt stress. Comparing the prediction accuracy of the 4 models, we evaluated the accuracy of the models using R^2, RMSE, and PA, and evaluated the model performance using Best Verification Performance and Time, as shown in Table 3. Although the PSO-BP (hln5) model has a fast convergence ability, among the four models, its R^2=0.839, RMSE=0.338, PA=84.61%, The accuracy is lower than that of ISHO-BP (hln5), so the comprehensive evaluation shows that the ISHO-BP (hln5) model performs better, R^2=0.952, RMSE=0.235, PA=89.30%, Best Verification Performance is 7 and time is 3s.

Table 3. The Estimation results of models with 5 hidden layer nodes based on BP algorithm.

Model	Dataset	Best Verification Performance（Round）	R^2	RMSE	PA	Time(s)
GA-BP(hln5)	Training set	10	0.968	0.186	91.53%	10
	Testing set		0.871	0.357	83.74%	
PSO-BP(hln5)	Training set	10	0.969	0.196	91.07%	7
	Testing set		0.839	0.338	84.61%	
SHO-BP(hln5)	Training set	25	0.957	0.213	90.30%	5
	Testing set		0.919	0.289	86.84%	
ISHO-BP(hln5)	Training set	7	0.948	0.239	89.12%	3
	Testing set		0.952	0.235	89.30%	

The following is the regression process of the BP neural network training fit of the four models, in which 100 groups are trained as training samples for the model, and the remaining 50 groups are evaluated as test sets for the accuracy of the experimental results. As shown in Figure 5, it is the regression curve of testing set. It is not difficult to see that all the four models have good fitting effect, among which the regression overfitting effect of BP neural network training fitting of ISHO-BP (hln5) model is the best.

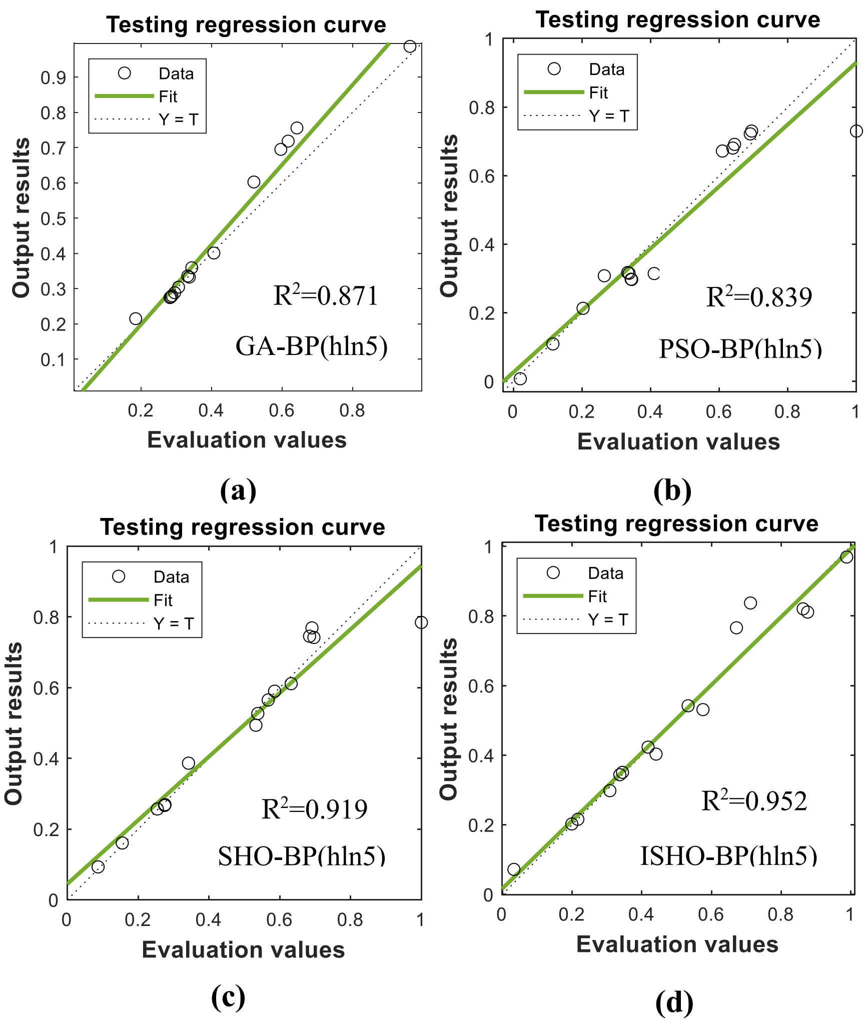

Figure 6.It is the regression curve of the testing set.

3.4. Comparison of Accuracy of Various Model Algorithms Based on the Number of Hidden Layer Nodes in BP Algorithm

To further verify that the change in the number of hln in the BP neural network affects the estimation ability of the model, we set BP neural networks with 10 and 15 hidden layer nodes respectively, and optimized them using genetic algorithm, particle swarm algorithm, hyena algorithm, and improved hyena algorithm, as shown in Table 4 and Table 5. The results indicate that different numbers of hln do affect the Estimation ability of the model. When the number of hln is 10, GA-BP (hln10)'s Best Verification Performance is better, ISHO-BP (hln10)'s R^2 is better, ISHO-BP (hln10)'s RMSE is less, ISHO-BP (hln10)'s PA is higher, and ISHO-BP (hln10)'s time is faster. Therefore, comprehensive evaluation shows that the ISHO-BP (hln10) model performs well, with relatively good R^2, RMSE, and PA values of 0.919, 0.267, and 87.84%, respectively.When the number of hidden layer nodes is 15, SHO-BP (hln15)'s Best Verification Performance is better, GA-BP (hln15)'s R^2 is better, PSO-BP (hln15)'s RMSE is less, PSO-BP (hln15)'s PA is higher, and ISHO-BP (hln15)'s time is faster. Overall evaluation shows that the PSO-BP (hln15)'s model performs relatively well, with a high prediction accuracy of 84.11%.

Table 4. The Estimation results of models with 10 hidden layer nodes based on BP algorithm.

Model	Dataset	Best Verification Performance	R^2	RMSE	PA	Time(s)

		（Round）				
GA-BP(hln10)	Training set	1	0.521	0.727	66.89%	19
	Testing set		0.675	0.554	74.77%	
PSO-BP(hln10)	Training set	5	0.917	0.294	86.61%	10
	Testing set		0.912	0.307	86.02%	
SHO-BP(hln10)	Training set	30	0.968	0.183	91.67%	15
	Testing set		0.825	0.405	81.56%	
ISHO-BP(hln10)	Training set	16	0.969	0.186	91.53%	5
	Testing set		0.919	0.267	87.84%	

Table 5. The Estimation results of models with 15 hidden layer nodes based on BP algorithm.

Model	Dataset	Best Verification Performance （Round）	R^2	RMSE	PA	Time(s)
GA-BP(hln15)	Training set	11	0.856	0.378	82.79%	50
	Testing set		0.892	0.351	84.02%	
PSO-BP(hln15)	Training set	14	0.927	0.286	86.98%	18
	Testing set		0.866	0.349	84.11%	
SHO-BP(hln15)	Training set	3	0.947	0.235	89.30%	11
	Testing set		0.621	0.659	69.99%	
ISHO-BP(hln15)	Training set	33	0.928	0.274	87.52%	7
	Testing set		-0.018	1.041	52.60%	

According to Tables 3, 4, and 5, it is not difficult to see that when the number of hln is 5, 10, and 15, the accuracy of GA-BP algorithm, PSO-BP model, SHO-BP model, and ISHO-BP model all exceed 52.60%. Overfitting occurs when the number of ISHO-BP model hidden layer nodes in the hidden layer is 15. This result proves that we should reduce the number of hln in BP neural network. In order to more intuitively represent the accuracy of the model, as shown in Figure 6, the determination coefficients, root mean square errors, and prediction accuracy histograms of the GA-BP model, PSO-BP model, SHO-BP model, and ISHO-BP model are presented. By comparing Figure 6, Table 3, Table 4, and Table 5, it is not difficult to see that the GA-BP model has better accuracy in the test set when the number of hln in the BP neural network is 15. The R^2, RMSE, and PA of GA-BP (hln15) are 0.892, 0.351, and 84.02%, respectively. The PSO-BP model has better accuracy in the test set when the number of hln in the BP neural network is 10. The R^2, RMSE and PA of PSO-BP (hln10) d are 0.912, 0.307, and 86.02%, respectively. The SHO-BP model has better accuracy in the test set when the number of hln in the BP neural network is 5, and the R^2, RMSE and PA of SHO-BP (hln5) are 0.912, 0.307 and

86.02%, respectively. The R^2, RMSE and PA are 0.919, 0.289 and 86.84%, respectively. The ISHO-BP model has better accuracy in the test set when the number of hln in the BP neural network is 5. The R^2, RMSE and PA of ISHO-BP (hln5) are 0.952, 0.235 and 89.30%, respectively. By comparing four better models, it was found that the determination coefficient of the ISHO-BP (hln5) model increased by 6.72% compared to the GA-BP (hln15) model, 4.39% compared to the PSO-BP (hln10) algorithm, and 3.59% compared to the SHO-BP (hln5) algorithm. The RMSE of the ISHO-BP (hln5) model decreased by 33.05% compared to the GA-BP (hln15) algorithm, 23.45% compared to the PSO-BP (hln10) algorithm, and 18.69% compared to the SHO-BP (hln5) algorithm. The accuracy of the ISHO-BP (hln5) model improved by 5.28% compared to the GA-BP (hln15) algorithm, 3.28% compared to the PSO-BP (hln10) model, and 2.46% compared to the SHO-BP (hln5) algorithm. Therefore, ISHO-BP (hln5) is the best model.

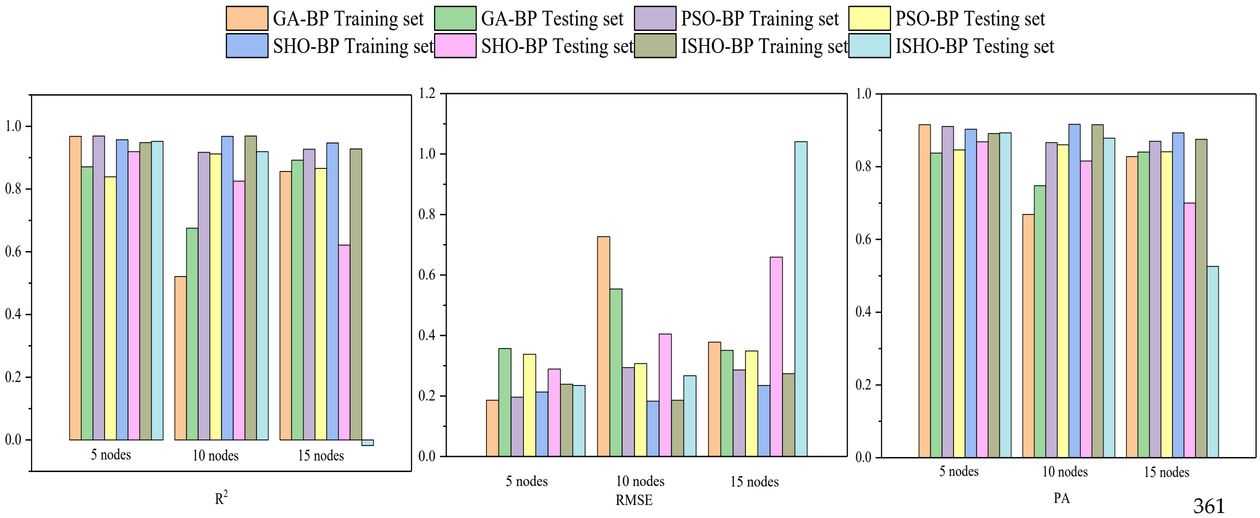

Figure 7. Model accuracy histograms of GA-BP algorithm, PSO-BP algorithm, SHO-BP algorithm, and ISHO-BP algorithm for four Estimation models with 5, 10, and 15 hidden layer nodes.

To further verify the performance of the four algorithms GA-BP (hln15), PSO-BP (hln10), SHO-BP (hln5), and ISHO-BP (hln5), the convergence curves of the four models were analyzed, as shown in Figure 8(b). It can be seen that the GA-BP (hln15) algorithm had the optimalconvergence speed, followed by the ISHO-BP (hln5) and SHO-BP (hln5) algorithm, and the PSO-BP (hln10) model had the worst convergence speed. Through comprehensive comparative evaluation and analysis, although convergence speed of ISHO-BP (hln5) algorithm is not as fast as that of the GA-BP (hln15) model, the ISHO-BP (hln5) algorithm shows the best prediction accuracy and can be determined as the cotton leaf area index Estimation model under Verticillium wilt stress.

Based on the comparative analysis of the experimental results, as shown in Figure 9，the ISHO-BP model demonstrates the most outstanding performance across all metrics, with its average accuracy (46.50%±2.46) significantly higher than the other three models. It particularly excels in recall (96.67%±7.45) and F1-score (96.08%±3.91), showcasing stronger stability and predictive capability while maintaining high precision (96.00%±5.48). Although the GA-BP model closely approaches ISHO-BP in accuracy (45.94%±1.52) and precision (95.78%±4.26), its recall and F1-score (94.30%±2.17) are slightly lower, indicating slightly weaker generalization ability. The PSO-BP and SHO-BP models perform relatively poorly—PSO-BP exhibits highly unstable accuracy (31.37%±12.31) and F1-score (80.00%±44.72), while SHO-BP, despite its high precision and recall (95.00%±11.18), suffers from notably low accuracy (34.08%±3.42). In terms of training efficiency, SHO-BP is the fastest (0.38 seconds), while ISHO-BP requires only 0.51 seconds, achieving a good balance between performance and efficiency. Overall, ISHO-BP delivers the best comprehensive performance and is well-suited for scenarios demanding high accuracy and stability.

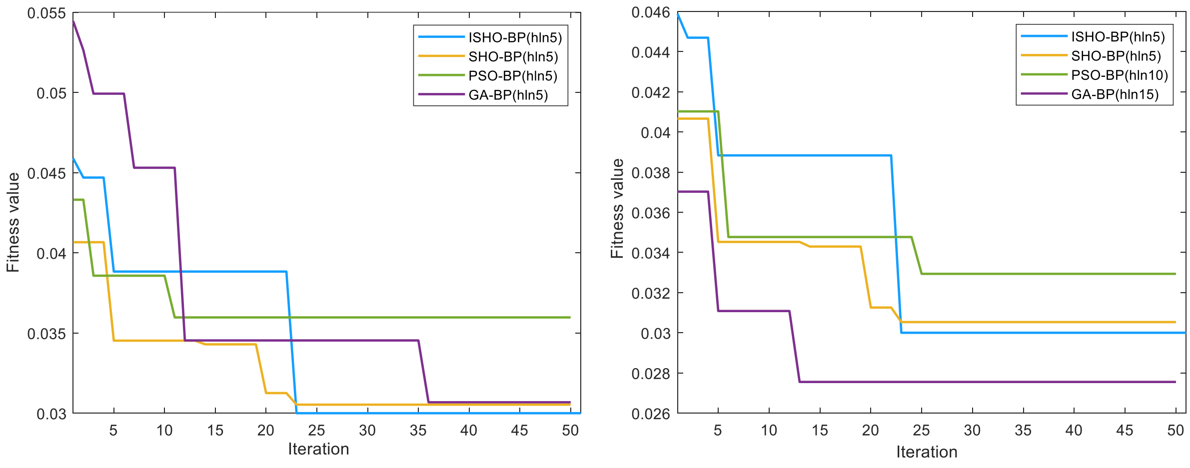

(a) (b)

Figure 8. (a) Iterative curves of GA-BP(hln5), PSO-BP(hln5), SHO-BP(hln5), and ISHO-BP. (hln5) models. (b) Iterative curves of GA-BP(hln15), PSO-BP(hln10), SHO-BP(hln5), and ISHO-BP(hln5) models.

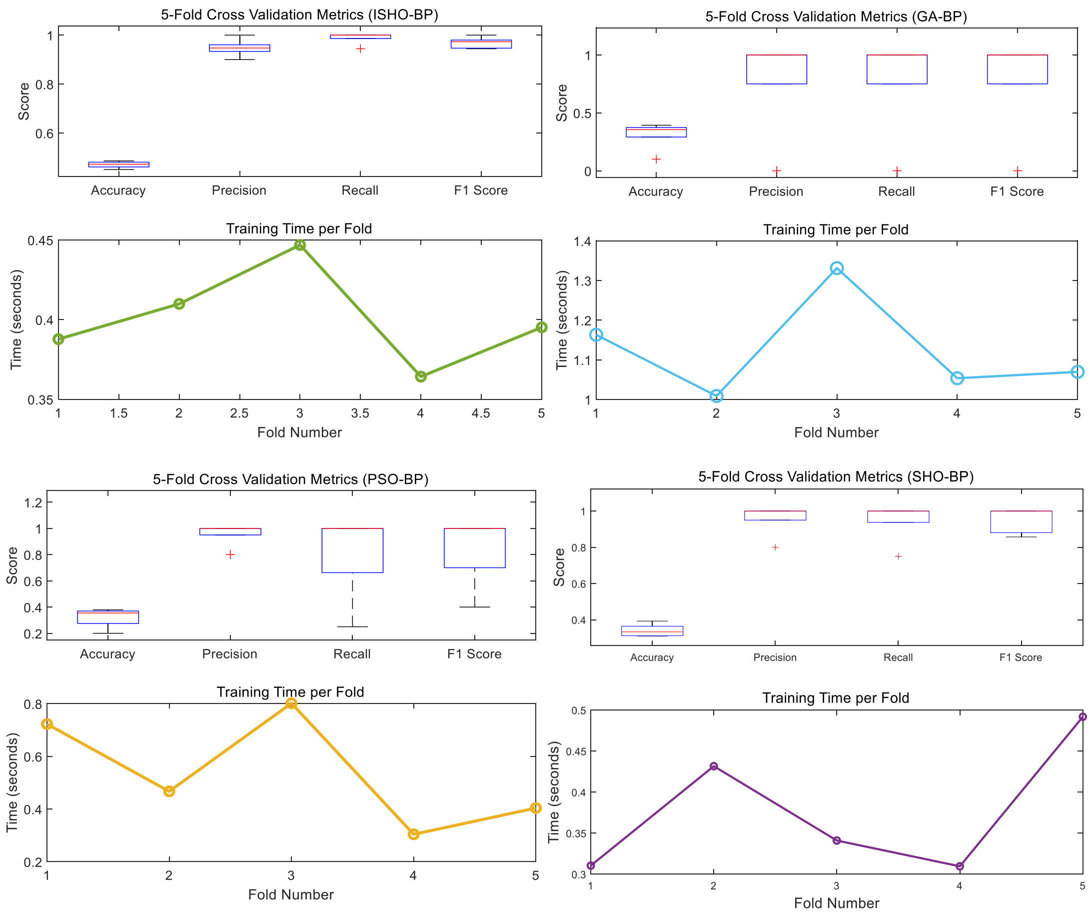

Figure 9. The 5-Fold Cross Validation Metrics and Training Time per Fold of GA-BP(hln15), PSO-BP(hln10), SHO-BP(hln5)and ISHO-BP(hln5) models.

3.5. Estimation of Cotton Leaf Area Index under Verticillium Wilt Stress Based on ISHO-BP Model

Four optimization models were used to optimize the number of hln of different BP neural networks, and the optimal models corresponding to the four models were obtained, and the accuracy of the models was higher than that of the number of other hln. Therefore, the optimal models corresponding to the four models, GA-BP(hln15), PSO-BP(hln10), SHO-BP(hln5), and ISHO-BP(hln5), were used to estimate the LAI of cotton under verticillium wilt stress, and the comparison between the predicted and the true value was obtained, as shown in Figure 8. It is not difficult to see that the estimation result of ISHO-BP (hln5) model is the best. Furthermore the results showed that the ISHO-BP model indeed exhibited good prediction performance, with a prediction error range of (-0.8, 0.5) and relative errors of less than 1.25%.

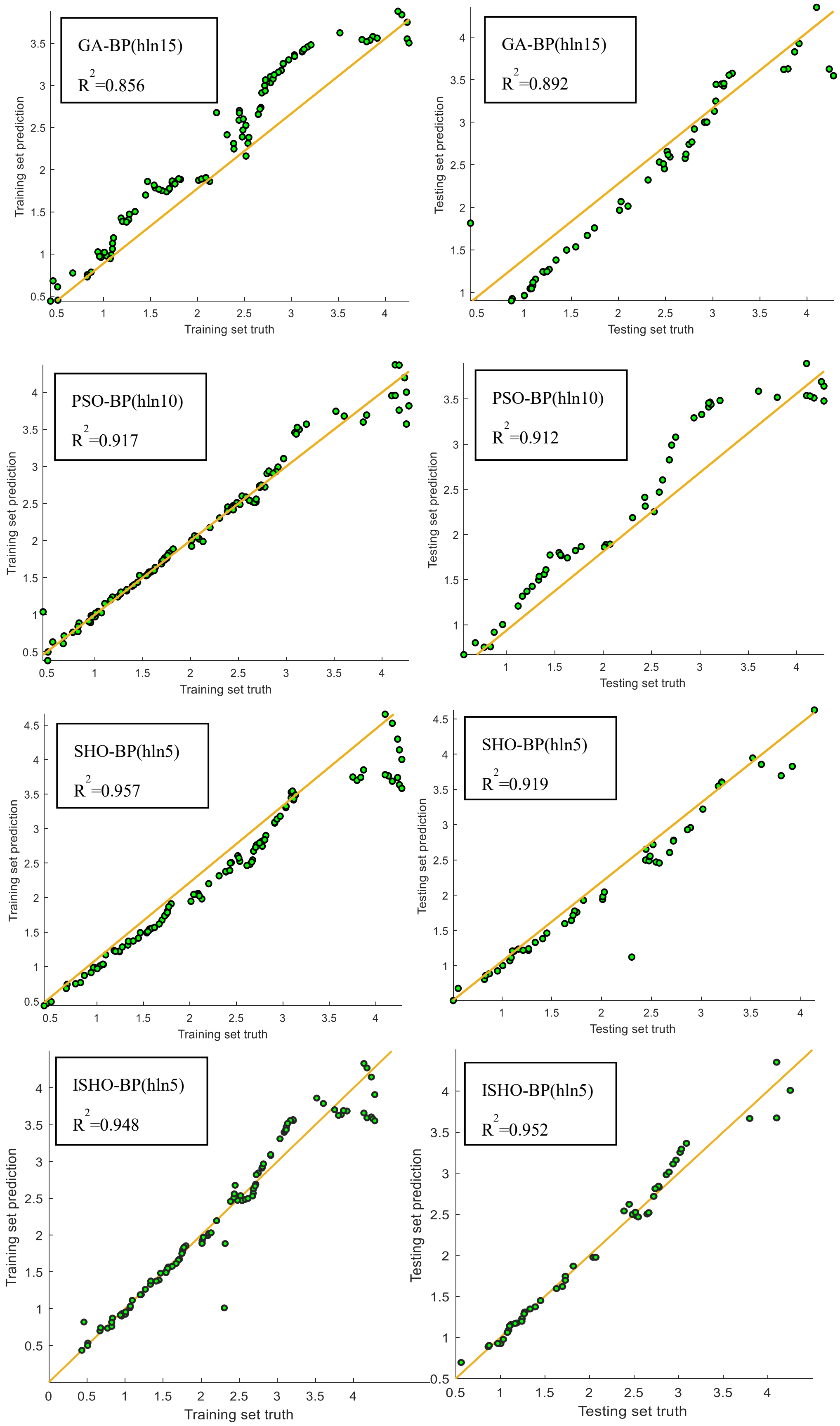

Figure 10. Estimation of cotton leaf area index under verticillium wilt stress based on four models

According to the above analysis results, the ISHO-BP (hln5) model had the best effect on estimating cotton leaf area index under verticillium wilt stress. The optimal model was used to estimate and map LAI of cotton under verticillium wilt stress, as shown in Figure 9. (a) was the spatial distribution map of LAI of cotton under verticillium wilt stress on August 31. (b) refers to the spatial distribution of LAI of cotton under the stress of verticillium wilt on September 14. From the perspective of spatial distribution, LAI on August 31 showed strip distribution, which was consistent with the cotton planting mode, while LAI was irregular on September 14 due to the influence of verticillium wilt. From the perspective of time distribution, LAI values on August 31 were on average greater than those on September 14, which was same with the onset of verticillium wilt when we collected the data. August 31 was the early stage of the disease, and September 14 was the middle stage of the disease.On August 31st, LAI values below 2.5 in partial cultivation areas indicated initial disease occurrence. By September 14th, most LAI values clustered around 3, while spatial distribution maps showed significantly expanded areas with LAI values below 2.5, exhibiting a "centrifugal diffusion" pattern that demonstrated significant correlation with increasing Verticillium wilt incidence. To further validate the universality of the ISHO-BP (hln5) model, the leaf area index of healthy cotton plants was estimated. The results are shown in Figure (c), which presents the spatial distribution characteristics of the leaf area index (LAI) of healthy cotton on August 29. It can be observed that the LAI values are relatively uniform, generally maintained between 4 and 6.These results were consistent with ground measurements, confirming progressive worsening of Verticillium wilt severity.It has provided technical support for the field management of Verticillium wilt., confirming progressive worsening of Verticillium wilt severity.It has provided technical support for the field management of Verticillium wilt.

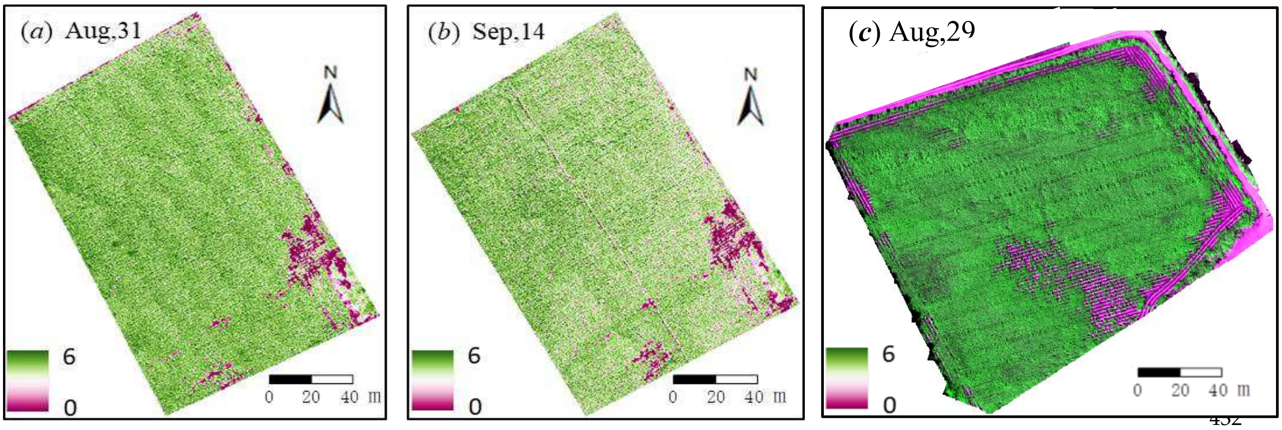

Figure 10. (a) was the spatial distribution map of LAI of cotton under verticillium wilt stress on August 31. (b) refers to the spatial distribution of LAI of cotton under the stress of verticillium wilt on September 14.(c) Spatial distribution map of leaf area index (LAI) for healthy cotton on August 29.

4. Discussion

4.1. Multispectral characteristic analysis of cotton under verticillium wilt stress

The application of multispectral remote sensing technology in farmland has been increasing, making rapid acquisition of vegetation information a viable option can. By measuring the spectral reflectance of plants, the severity of crop diseases and pests can be observed. Researchers studying rice blast reports have confirmed that there are differences in the NIR spectral reflectance data presented by different severity of rice blast disease (Guo et al., 2019). If the blast disease is severe, the spectral reflectance of the leaves is low, and vice versa. The spectral reflectance of wheat stripe rust was also studied that different degrees of stripe rust damage has a "peak" on the "green edge" and a "valley" on the "red edge", and in the near-infrared spectral range (Ma et al.,2 021). The spectral reflectance of wheat will decrease significantly if the disease severity increases(Song et al.,2022), a study on Verticillium wilt found that using hyperspectral data to invert the disease severity of cotton single leaf resulted in a fitting value of over

0.68 and a prediction accuracy of 83.56% (Chen et al., 2010). The UAV multi-spectral data was used to estimate the cotton LAI under verticillium wilt stress, and the goodness of fit of algorithm reached 0.952. In summary, the use of multispectral data has proved to be a viable method for estimating cotton leaf area index, especially under adverse conditions caused by verticillium wilt.

4.2. Performance Comparison of Different Optimization Algorithms under Different Numbers of Hidden Layer Nodes

The BP neural network model demonstrates strong nonlinear mapping capabilities and flexible architecture, yet suffers from slow convergence (often requiring hundreds to thousands of iterations) and susceptibility to local optima, prompting the need for metaheuristic optimization approaches. This study's comprehensive evaluation of GA-BP, PSO-BP, SHO-BP, and ISHO-BP algorithms (Figures 6-9, Tables 3-5) reveals that while ISHO-BP (hln5) achieves superior predictive performance (R^2=0.952, RMSE=0.235, PA=89.30%), this comes with nuanced tradeoffs: GA-BP (hln15) shows faster iteration but poorer generalization (17% lower R^2) and longer runtime, suggesting an accuracy-efficiency paradox in hidden layer configuration. The results confirm (Ma et al., 2010) findings while extending them through three critical insights: (1) hybrid optimization (ISHO-BP) effectively mitigates BP's traditional limitations but introduces marginal computational overhead (0.51s vs GA-BP's 0.44s); (2) the optimal hln5 configuration challenges conventional wisdom about node quantity-performance relationships; (3) algorithm performance exhibits nonlinear interactions with network architecture, where PSO-BP's instability (F=5.97, P>0.05) and SHO-BP's moderate results underscore the importance of balancing exploration and exploitation. These findings suggest that while ISHO-BP represents the most balanced solution for precision-critical applications, GA-BP may still hold value for scenarios prioritizing rapid prototyping, highlighting the need for context-aware algorithm selection based on specific operational constraints and accuracy requirements.

Compared with Chen Bing and others who used empirical models to inverse the pigment content of cotton leaves under pest and disease stress using hyperspectral, the error was increased by 0.05% (Chen et al., 2024); According to Table 3, using the ISHO-BP model compared with the linear model applied by (Jing et al., 2009). In the high-yield crop research area of Xinjiang crop field in Shihezi University, this method represents a significant improvement in accuracy. Ma et al. evaluated the severity of wilt by combining the Verticillium wilt index, color index, and texture features. Their results showed that using multiple data sources for collaborative modeling had the highest accuracy (R^2: 0.65-0.88) (Ma et al; 2024). Compared with this study, the estimation accuracy is similar, but slightly lower. The main reason why our research results are better than others is: (1) the degree of matching between multispectral remote sensing data and ground data collection (Ma et al., 2024; Zou et al., 2006;); (2) The selection of multiple vegetation index combinations for estimating LAI has played a complementary role (Ji et al.,2022).

4.3. Limitations and perspectives

Multispectral data of the canopy of cotton verticillium wilt plant Tahe No. 2 were collected. The inverse model of cotton leaf area index under verticillium wilt stress based on BP algorithm and several optimization algorithms was established by preprocessing multi-spectral data. The results are shown in Figure 6, Figure 7, Figure 8, Table 3, Table 4 and Table 5. The research results show that the ISHO-BP (hln5) algorithm obtains the best estimation performance with the shortest algorithm running time. The spatial distribution diagram of LAI obtained by using the ISHO-BP (hln5) algorithm is shown in Figure 9. The results show that the distribution of LAI observed both spatially and spatially is consistent with the actual cotton growth status.

(1)However, this study only examined multispectral data under verticillium wilt stress of specific cotton varieties. Therefore, to ensure the reliability and precision of the ISHO-BP algorithm in estimating cotton leaf area index under Verticillium wilt stress conditions, future studies should consider more cotton varieties, planting methods and cotton growth periods.

(2) Under Verticillium wilt stress, the cotton leaf area index estimation was the central focus of this research. The studies afterwards, the multi-spectral data obtained by UAV can be used for accurate estimation and identification of cotton leaf area index under disease and pest stress based on ISHO-BP model. The farmland can be monitored in real time, and the corresponding management plan can be formulated to meet diverse needs s of cotton farmers, increase the income of cotton farmers, and promote economic development.

5. Conclusions

How to quickly understand the crop disease situation and implement corresponding measures is the key to promote the high-quality development of agriculture in southern Xinjiang. Multispectral data of cotton canopy affected by verticillium wilt were analyzed. The correlation between vegetation index and leaf area index of cotton was analyzed and four models, GA-BP, PSO-BP, SHO-BP and ISHO-BP were established. By setting different number of hidden nodes in BP neural network, the determination coefficient, root mean square error and prediction accuracy of 12 models are obtained with good results. The more hln in the BP neural network, the better the accuracy of the algorithm is not necessarily. The more nodes in the hidden layer, the overfitting phenomenon may occur, such as ISHO-BP (hln15).The best algorithm in the GA-BP algorithm is GA-BP (hln15), the best algorithm in the PSO-BP algorithm is PSO-BP (hln10), the best model in the SHO-BP model is SHO-BP (hln5), and the best model in the ISHO-BP model is SHO-BP (hln5). Compared with the prediction accuracy of the four optimal models, the error range of ISHO-BP (hln5) model estimation is (-0.8,0.5), R^2, RMSE and PA are 0.952, 0.235 and 89.30%, respectively and the best results are obtained and the running time is short.Under the ISHO-BP (hln5) model, the spatial distribution patterns of leaf area index (LAI) in cotton—both under Verticillium wilt stress and in healthy plants—exhibit high consistency with actual field observations.It is confirmed that the estimation with the ISHO-BP (hln5) model is satisfactory. Therefore, the ISHO-BP (hln5) model is suitable for high-precision estimation of cotton LAI under verticillium wilt stress in this study. It is expected that the model can also obtain satisfactory results in crop LAI estimation under pests and diseases stress other than this study.

Author Contributions: Y.T. is responsible for Writing and original draft preparation; formal analysis, J.H.; investigation, N.Z.; software verification, M.S.; visualization, L.W.; conceptualization, methodology, project administration, Q.J. All the authors shared the article and agreed to publish it

Funding: This research was partially funded by [the Tarim University President's Fund of HuYang Talent Cultivation Research Initiation Project] grant number [2026133], [National Natural Science Foundation Project of Regional Science Fund] grant number [62061041], [National Natural Science Foundation Project of Youth Fund] grant number [32101621] and [The "Qiangnan" Science and Technology Innovation Backbone Talent Plan Project of the Xinjiang Production and Construction Corps] grant number [2022CB001-05],Tarim University first-class course construction project(Mathematical Modeling) grant number [TDYLKC202430].

Conflicts of Interest: The authors declare that they have no known competing financial interest or personal relationships that could have appeared to influence the work reported in this paper.
Consent to Publish declaration: not applicable
Ethics and Consent to Participate declarations: not applicable

References

Aziguli AS. The challenges and solutions of China's cotton industry. Jiangxi Agric. 2016;1.

Bonah E, Huang X, Yi R, Aheto JH, Yu S. Vis-NIR hyperspectral imaging for the classification of bacterial foodborne pathogens based on pixel-wise analysis and a novel CARS-PSO-SVM model. Infrared Phys Technol. 2020;105:103220. doi:10.1016/j.infrared.2020.103220

Chen B. Research on remote sensing monitoring of cotton Verticillium wilt based on multi-platform. Shihezi University; 2010.

Chen B, Li SK, Wang KR. Hyperspectral remote sensing estimation of pigment content in cotton leaves under disease stress. Spectrosc Spectr Anal. 2010;30:421 – 425.

Chen JM, Black TA. Defining leaf area index for non-flat leaves. Plant Cell Environ. 1992;15:421 – 429. doi:10.1111/j.1365-3040.1992.tb00992.x

Chen PC, Zhang JH, Lei YH, Li MM. Research progress on hyperspectral remote sensing monitoring of crop diseases and pests. Chin Agric Bull. 2006;02:388 – 391.

Dai TH, Sun CX, Huang JP. Hyperspectral band selection based on golden sine chaotic spotted hyena optimization algorithm. Adv Laser Optoelectron. 2022;59:519 – 528.

Dhiman G, Kaur A. Spotted hyena optimizer for solving engineering design problems. In: Proceedings of the 2017 International Conference on Machine Learning and Data Science (MLDS). Noida, India; 2017:114 – 119.

Dilixiati YMM. Research on cotton pest monitoring based on multispectral remote sensing images of drones. Xinjiang University; 2021.

Fitzgerald G, Rodriguez D, O'Leary G. Measuring and predicting canopy nitrogen nutrition in wheat using a spectral index—The canopy chlorophyll content index (CCCI). Field Crops Res. 1975;116:318 – 324. doi:10.1016/j.fcr.2010.01.010

Gao C, Ji X, He Q. Monitoring of wheat fusarium head blight on spectral and textural analysis of UAV multispectral imagery. Agriculture. 2023;13(2):293. doi:10.3390/agriculture13020293

Gao L, Yang GJ, Wang BS. Research on the estimation of soybean leaf area index based on unmanned aerial vehicle remote sensing images. Chin J Ecol Agric. 2015;23:868 – 876.

Gitelson AA, Kaufman YJ, Merzlyak MN. Use of a green channel in remote sensing of global vegetation from EOS-MODIS. Remote Sens Environ. 1996;58:289 – 298. doi:10.1016/S0034-4257(96)00072-7

Gonsamo A, Pellikka P. Methodology comparison for slope correction in canopy leaf area index estimation using hemispherical photography. For Ecol Manag. 2008;256:749 – 759. doi:10.1016/j.foreco.2008.05.026.

Guo W, Zhu Y, Wang H, Zhang J, Dong P, Qiao H. Monitoring model of winter wheat take-all based on UAV hyperspectral imaging. Trans Chin Soc Agric Mach. 2019;50:162 – 169.

Hong ZY. Research on the inversion method of forest leaf area index based on remote sensing images. Northeast Forestry University; 2022.

Huang CL, Dun JF. A distributed PSO – SVM hybrid system with feature selection and parameter optimization. Appl Soft Comput. 2008;8:1381 – 1391. doi:10.1016/j.asoc.2007.10.012.

Huang MY, Wang JH, Huang YD, Huang WJ, Zhao CJ, Liu LY. Research progress on hyperspectral remote sensing monitoring of winter wheat stripe rust (review). J Anhui Agric Univ. 2004;01:119 – 122.

Hunt ER, Daughtry C, Eitel JU, Long DS. Remote sensing leaf chlorophyll content using a visible band index. Agron J. 2011;103:1090 – 1099. doi:10.2134/agronj2010.0395

Ji S, Gu C, Xi X, Zhang Z, Hong Q, Huo Z, Zhao H, Zhang R, Li B, Tan C. Quantitative monitoring of leaf area index in rice based on hyperspectral feature bands and ridge regression algorithm. Remote Sens. 2022;14(12):2777. doi:10.3390/rs14122777

Jian GL, Zou YF, Ma C. The reasons and countermeasures for the continuous prevalence of cotton wilt disease. Chin Cotton. 2003;30:2.

Jing X, Huang WJ, Wang JH. Study on hyperspectral inversion model for severity of Verticillium wilt in cotton leaves. Spectrosc Spectr Anal. 2009;29:3348 – 3352.

Jordan CF. Derivation of leaf-area index from quality of light on the forest floor. Ecology. 1969;50:663 – 666. doi:10.2307/1936256

Lai NN. Screening, identification, and efficacy study of antagonistic actinomycetes against cotton wilt in Xinjiang. Shihezi University; 2014.

Li DH. Runoff prediction based on PCA-SHO-SVM and PCA-SHO-BP models. J Water Resour Water Eng. 2021;32:97 – 102.

Li L, Ustin SL, Riano D. Retrieval of fresh leaf fuel moisture content using genetic algorithm partial least squares (GA-PLS) modeling. IEEE Geosci Remote Sens Lett. 2007;4:216 – 220. doi:10.1109/LGRS.2006.888104

Li S, Lin Y, Zhu P, Jin L, Bian C, Liu J. Combining UAV multispectral imaging and PROSAIL model to estimate LAI of potato at plot scale. Agriculture. 2022;14(12):2159. doi:10.3390/agriculture14122159

Li TB, Hu JH, Zhou QK. Infrared image segmentation based on improved spotted hyena optimization algorithm. Infrared Technol. 2021;43:994 – 1002.

Liu HY, Wang W, Zhang RF. Overview of cotton Verticillium wilt in major cotton regions of Xinjiang. Plant Prot. 2015;41:138 – 142.

Ma C. Research on cotton wilt and Verticillium wilt. Res Cotton Wilt Verticillium Wilt; 2007.

Ma CS. The causes and prevention measures of the major occurrence of cotton wilt disease in 1993. Chin Agric Bull. 1994;10:3.

Ma H, Huang W, Dong Y, Liu L, Guo A. Using UAV-based hyperspectral imagery to detect winter wheat fusarium head blight. Remote Sens. 2021;13:3024. doi:10.3390/rs13153024

Ma R, Zhang NN, Zhang X, Bai TC, Yuan XT, Bao H, He DD, Sun WJ, He Y. Cotton Verticillium wilt monitoring based on UAV multispectral-visible multi-source feature fusion. Comput Electron Agric. 2024;217:108628. doi:10.1016/j.compag.2023.108628

María Luisa E, Frédéric B, Marie W. Slope correction for LAI estimation from gap fraction measurements. Agric For Meteorol. 2008;148:1553 – 1562. doi:10.1016/j.agrformet.2008.05.005

Monteith J, Unsworth M. Principles of environmental physics: plants, animals, and the atmosphere. Academic Press; 2013.

Nkongolo M, VanDeventer JP, Kasongo SM, Zahra SR, Kipongo J. A cloud-based optimization method for zero-day threats detection using genetic algorithm and ensemble learning. Electronics. 2022;11:1749. doi:10.3390/electronics11111749

Nie X, Aini N, Tian X, Han P, Zhu L, Lin Z. Cotton ethylene response factor GhERF91 is involved in the defense against Verticillium dahliae. J Integr Agric. 2024;23(10):1 – 12. doi:10.1016/j.jia.2023.07.022

Pearson RL, Miller LD. Remote mapping of standing crop biomass for estimation of the productivity of the shortgrass prairie. In: Proceedings of the 8th International Symposium on Remote Sensing of the Environment. Ann Arbor, Michigan, USA; 1972:1355 – 1379.

Qi DH, Kang JC. Design of BP neural network. Comput Eng Des. 1998;02:010.

Rumelhart DE, McClelland JL. Parallel distributed processing: explorations in the microstructure of cognition. Vol. 1. MIT Press; 1986.

Saremi S, Mirjalili S, Lewis A. Grasshopper optimisation algorithm: theory and application. Adv Eng Softw. 2017;105:30 – 47. doi:10.1016/j.advengsoft.2017.01.004

Shao GM, Wang YJ, Han WT. Estimation method of summer maize leaf area index based on unmanned aerial vehicle multispectral remote sensing. Smart Agric. 2020;2:118.

Smith NJ, Clark E. Estimating salal leaf area index and leaf biomass from diffuse light attenuation. Can J For Res. 1990;20:1265 – 1270. doi:10.1139/x90-168

Song L, Liang Q, Chen H, Hu H, Luo Y, Luo Y. A new approach to optimize SVM for insulator state identification based on improved PSO algorithm. Sensors. 2022;23:272. doi:10.3390/s23010272

Tan YB, Zhao ZH. Main measurement methods for leaf area index. For Surv Plan. 2008;33:45 – 48.

Tao H, Xu L, Feng H, Yang G, Dai Y, Niu Y. Estimation of plant height and leaf area index of winter wheat based on UAV hyperspectral remote sensing. Trans Chin Soc Agric Mach. 2020;51:193 – 201.

Wang Y. Research on the inversion method of wheat leaf area index based on unmanned aerial vehicle remote sensing. Northwest A&F University; 2017.

Wang ZY, Liu T, Zhang H. Construction of wheat rust estimation model based on multispectral image features. J Henan Agric Univ. 2023;57:826 – 834.

Watson DJ. Comparative physiological studies on the growth of field crops: I. variation in net assimilation rate and leaf area between species and varieties, and within and between years. Ann Bot. 1947;11:41 – 76. doi:10.1093/oxfordjournals.aob.a083148

Wilson JW. Inclined point quadrats. New Phytol. 1960;59:1 – 7. doi:10.1111/j.1469-8137.1960.tb06200.x

Xue HZ, Wang CJ, Zhou HM. Estimation of high-resolution leaf area index by BP neural network model based on simulated annealing algorithm. Remote Sens Technol Appl. 2019;35:1057 – 1069.

Yang S, Hu L, Wu H. Estimation model of winter wheat yield based on UAV hyperspectral data. In: *IGARSS 2019-2019 IEEE International Geoscience and Remote Sensing Symposium*. IEEE; 2019:7212 – 7215.

Yin G, Cao B, Li J. Path length correction for improving leaf area index measurements over sloping terrains: a deep analysis through computer simulation. IEEE Trans Geosci Remote Sens. 2020;58:4573 – 4589. doi:10.1109/TGRS.2020.2965308

Zhang GL, Li QS, Tian YS, Zhao ZQ, Ma PP, Yu H, Xie ZM. A new method for rapid indoor identification of cotton seedling resistance to Verticillium wilt—non-woven seedling bag inoculation method. Northwest Agric J. 2018;27:155 – 162.

Zhang Y, Wang XF, Ding ZG. Transcriptome profiling of Gossypium barbadense inoculated with Verticillium dahliae provides a resource for cotton improvement. BMC Genomics. 2013;14:637. doi:10.1186/1471-2164-14-637

Zhao D, Feng S, Cao Y, Yu F, Guan Q, Li J, Zhang G, Xu T. Study on the classification method of rice leaf blast levels based on fusion features and adaptive-weight immune particle swarm optimization extreme learning machine algorithm. Front Plant Sci. 2022;13:879668. doi:10.3389/fpls.2022.879668

Zhao X, Li MC, Mei L. The occurrence and control measures of cotton wilt disease in Alar Reclamation Area, Xinjiang. China Cotton. 2021;48.

Zhong L, Zhou Y, Zhou G, Luo Q. Enhanced discrete dragonfly algorithm for solving four-color map problems. Appl Intell. 2023;53:6372 – 6400. doi:10.1007/s10489-022-03914-5

Zou XF, He QH, He JL. The current development status and related technologies of unmanned aerial vehicles. Aerial Missile. 2006;9 – 14.

Zou X, Zhu S, Mõttus M. Estimation of canopy structure of field crops using Sentinel-2 bands with vegetation indices and machine learning algorithms. Remote Sens. 2022;14(12):2849. doi:10.3390/rs14122849

Zhang H, Wang G, Song F, Wen Z, Li W, Tong L, Kang S. Improving chili pepper LAI prediction with TPE-2BVIs and UAV hyperspectral imagery. Comput Electron Agric. 2025;235:110368. doi:10.1016/j.compag.2025.110368

Feng H, Fan Y, Yue J, Bian M, Liu Y, Chen R, Ma Y, Fan J, Yang G, Zhao C. Estimation of potato above-ground biomass based on the VGC-AGB model and deep learning. Comput Electron Agric. 2025;232:110122. doi:10.1016/j.compag.2025.110122

Zhang H, Li W, Wang G, Song F, Wen Z, Zhang H, Tong L, Kang S. Predicting stomatal conductance of chili peppers using TPE-optimized LightGBM and SHAP feature analysis based on UAVs’ hyperspectral, thermal infrared imagery, and meteorological data. Comput Electron Agric. 2025;231:110036. doi:10.1016/j.compag.2025.110036